ChemPubSoc Europe

DOI: 10.1002/open.201800222

Open Access ChemistryOPEN Communications

Anthraquinone Derivative Reduces Tau Oligomer Progression by Inhibiting Cysteine-Cysteine Interaction

Carlos Areche,[a] Francisca Zapata,[c] Mathias González,[c] Esteban Díaz,[c] Rubén Montecinos,[b] Marcos Hernández,[a] Francisco Melo,[b] and Alberto Cornejo*[c]

Tau protein is a natively unfolded protein whose primary role is to participate in axonal transport closely associated with microtubules. Neurodegenerative disorders including Alzheimer's disease and Tauopathies involved tau protein that is found hyperphosphorylated *in vivo;* then, tau is detached from microtubules to form toxic aggregates or oligomers, which have a deleterious effect on membranes, triggering an inflammatory response. Considering finding tau inhibitors, we isolated two compounds in the ethyl acetate extract from *Xanthoria ectaneoides* (Nyl.) Zahlbr; ergosterol peroxide (**1**) and a new anthraquinone (**2**). We established the structure through spectroscopic data and biogenic considerations, and we named it "2-hydroxy-3-((8-hydroxy-3-methoxy-6-methylanthraquinonyl) oxy)propanoic acid". This new anthraquinone was evaluated as a tau inhibitor by ThT fluorescence, dot blot assays and total internal reflection fluorescence microscopy. Our results strongly suggest that this anthraquinone remodels soluble oligomers and diminishes β-sheet content. Moreover, through the fluorescence labeling of cysteine inside of the microtubule-binding domain (4R), we showed that this anthraquinone could reduce the oligomers progression by inhibiting cysteine interactions.

Alzheimer's disease (AD) is the most prevalent form of dementia,[1] involving beta-amyloid (Aβ) and microtubule-associated protein tau. The proteins deposition are characterized for plaques and neurofibrillary tangles respectively (NFT).[2] Tau protein participates in axonal transport and microtubule stability however once tau is hyperphosphorylated, it detaches from microtubules and starts to form aggregates in soma and dendrites of neuron cells.[3] Moreover, tau protein is involved in related neurodegenerative disorders such as tauopathies, which includes progressive nuclear palsy (PSP), corticobasal degeneration (CBD) Pick's disease, argyrophilic grain disease (AGD), and frontotemporal dementia (FTP).[4] Tau pathology involving the microtubule-binding domain (4R) is associated with PSP, CBD, and AGD; where tau aggregates can be found in the medial temporal lobe, cortex, basal ganglia, subthalamic nucleus, and substantia nigra.[4] Tau is an unfolded protein whose structure has two fibril-forming motifs, ^{275}VQIINK^{280} and ^{306}VQIVYK^{311}.[5] Hence, to form the fibrillar structure of tau, it is required the addition of polyanions such as heparin which suggests an essential role of electrostatic interaction to form both fibrils or aggregates.[6] These two motifs are within the microtubule-binding domain (4R) of tau and are prone to form cross β structure.[7] Moreover, two Cysteines have a central role in polymerization as well.[8] The first step of aggregation occurs by forming a covalent bond between Cysteine residues to form soluble oligomers.[9] Interestingly, the first stage of oligomers formation is possible to find a mixture of random coil and β sheet. However, as long the polymerization of tau occurs, mature oligomers are formed whose content is majority β sheet content.[10] These oligomers structures are detected at the prefrontal cortex in Braak stage I.[11] Moreover, the pathological hallmark of AD are extracellular deposits of β-amyloid (Aβ) and intracellular inclusions of tau protein.[12] Thus, these neuropathological features have strongly influenced the therapeutic strategies, whose primary focus is Aβ. The amyloid hypothesis relies on the fact that Aβ accelerates the NFT formation and neuronal death in the neocortex.[13] However, all these approaches focused on Aβ, including clinical trials have failed since there are no cognitive improvements in patients with AD.[14] Besides tau is related to FTD linked to chromosome 17 where the neuronal loss occurs in the absence of Aβ.[15] Thus, considering that tau correlates better with cognitive impairment and dementia symptoms, the focus of drug discovery strategies are pointing tau.[16] Accordingly, the therapeutic approaches focused on tau involved monoclonal antibodies, kinase inhibitors, a microtubule stabilizer, selective serotonin acetylcholinesterase reuptake inhibitors, and tau inhibitors. Interestingly it has been described that small compounds can interact with tau by inhibiting Cysteine interactions promoting the formation of incompetent aggregate forms.[17] Interestingly, anthraquinones inhibitors have demonstrated that can reduce progression of tau aggregation in cells.[18] Lichens are symbiotic associations between heterotrophic fungi and algae and cyanobacteria. A peculiarity of lichen is its remarkable ability to

[a] *Dr. C. Areche, M. Hernández*
Departamento de Química, Facultad de Ciencias
Universidad de Chile
Las Palmeras 3425, 7800003, Santiago-Chile
[b] *R. Montecinos, Dr. F. Melo*
Departamento de Física
Avenida Ecuador 3493, 9170124, Santiago-Chile
[c] *F. Zapata, M. González, E. Díaz, Dr. A. Cornejo*
Escuela Tecnología Médica, Facultad de Medicina
Sazie 2315, 8370092 Santiago-Chile
E-mail: alberto.cornejo@unab.cl

Supporting information for this article is available on the WWW under https://doi.org/10.1002/open.201800222

tolerate extreme atmospheric conditions such as alpine zone, arctic habitat, and Antarctic region. These stressful environmental conditions are responsible for the diversity of secondary metabolites produced.[19] Lichen substances are synthesized via polymalonyl, shikimate, and mevalonic acid pathway bringing unique structures of secondary metabolites such as phenolic compounds, dibenzofurans, depsides, depsidones, responses, quinones, and pulvinic acid derivatives.[20] Here, we demonstrated that a new Anthraquinone-derivative inhibits fibrillization via Cysteine-Cysteine interaction, besides oligomers are structurally remodeled after treatment with 2. Given that there is just palliative treatment for Alzheimer's and Tauopathies it is crucial to considered new compounds as a scaffold for neurodegenerative disorders.

From an EtOAc extract of *X. ectaneoides*, ergosterol peroxide **1** and the new compound **2** were isolated and identified based on its spectroscopic analysis. The structure of ergosterol peroxide we confirmed by comparing the spectroscopic data with those from the literature.[21] The compound **2** was isolated as a yellow gum and had a molecular formula of $C_{19}H_{16}O_8$ according to NMR and HRESIMS data ([M−H]=371.0773) (Figure S1 and Figure S2 respectively). The ^{1}H-NMR spectrum showed the presence of a singlet at 2.20 ppm assigned to the aromatic methyl group and a singlet at 4.02 ppm assigned to a methoxy group attached to the aromatic ring. Also, the presence of four doublets in the aromatic region at 7.83 brs (H-4), 7.38 d (2.5 Hz, H-5), 7.30 brs (H-2) and 6.82 d (2.5 Hz, H-7) was consistent with an anthraquinone moiety. These data of compound 2 was close to that of parietin, differing mainly by the presence of two signals at 5.30 dd, 4.84 d and 4.03 d indicating a hydroxypropanoic acid group linked to C-8. The ^{13}C NMR spectrum showed the presence of 19 carbons, instead of 16 carbons seen for parietin. The IR spectrum showed absorption bands at 3400–2500 and 1700 cm^{-1}, indicating the presence of COOH group. HMBC correlations assigned the position of the hydroxypropanoic acid chain. In HMBC spectrum (Scheme 1), the proton signal at δ 6.82 (H-7) showed long-range correlations with the carbon signals at C-8, C-3′ and C-2′ indicating that the hydroxypropanoic acid group was at C-8. Also, the proton signal at δ 4.84 (H-3′) correlated with C-8, C-1′ and C-2′ confirming this side chain at C-8. 2D TOCSY experiment on **2** showed a clear correlation between H-3′ and H-2′ confirming the hydroxypropanoic acid residue. The spectroscopic data of **2** were very similar to those reported for the synthetic product 3-(1,8-dihydroxy-6-methoxy-9,10-anthraquinon-3-yl) propionic acid. Thus, we identified and described the compound **2** as 2-hydroxy-3-((8-hydroxy-3-methoxy-6-methylanthraquinonyl)oxy)propanoic acid for the first time. Biosynthetically, lichen substances are derived from three chemical pathways: acetate-polymalonate, shikimate and mevalonate pathway. Anthraquinones are produced by the acetate-polymalonate pathway. Thus, the hydroxypropionic acid residue of compound **2** could be derived from the nucleophilic attack of the OH at C-8 to the phosphoenolpyruvate (PEP), to give **2**, as shown in Figure S3.

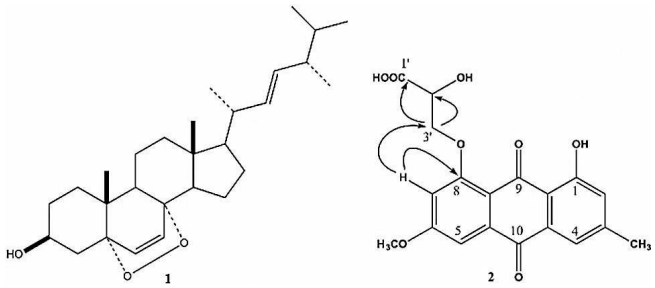

Scheme 1. Overview of the structures **1** and **2** (HMBC correlation).

2 was isolated and evaluated as tau aggregation inhibitor by ThT fluorescence assay to determine inhibition properties. First, we try to determinate the β sheet formation by monitoring the aggregation of tau 4R (Figure S4). We found that at 48 h the aggregation experiment ThT signal was higher suggesting an increasing β sheet amount (Figure 1A). Thus, we decided to test whether this anthraquinone could inhibit the aggregation process. Compound **2** inhibited the transition from soluble oligomers to aggregated protein at 100 μM concentration (Figure 1B). According to our data, the compound **2** inhibits nearly 20% of the aggregation process of tau.

Moreover, we decided to monitor the aggregation by total internal reflection fluorescence microscopy (TIRFM). Hence, we

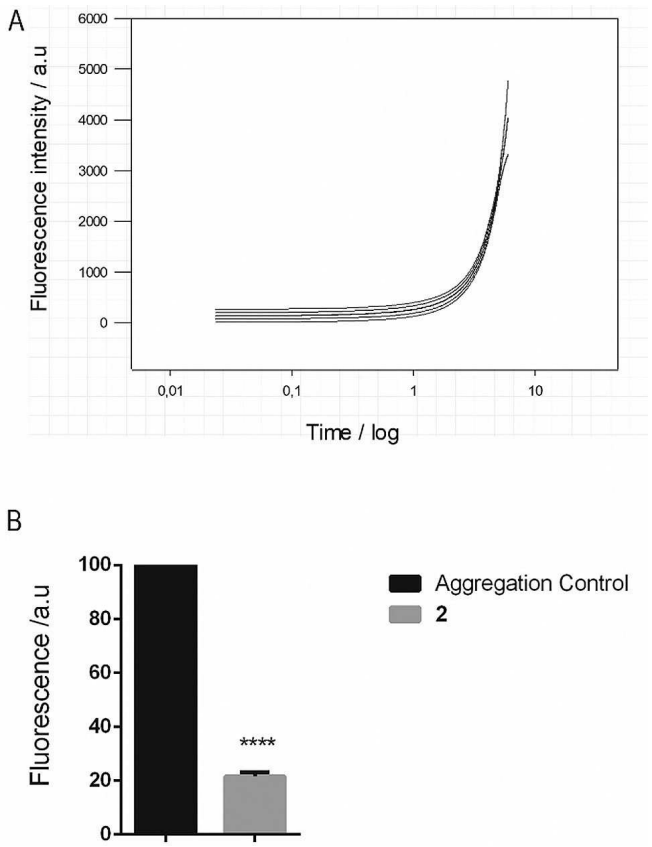

Figure 1. A) Aggregation process monitored by ThT fluorescence at 48 h. Non-linear regression dynamic fitting. Fitting represents the regression line (black) and confidence limit 95% (red line). B) Aggregation process (48 h) inhibited by **2** at 100 μM. P values were determined by *t*-student test $P < 0.05$.

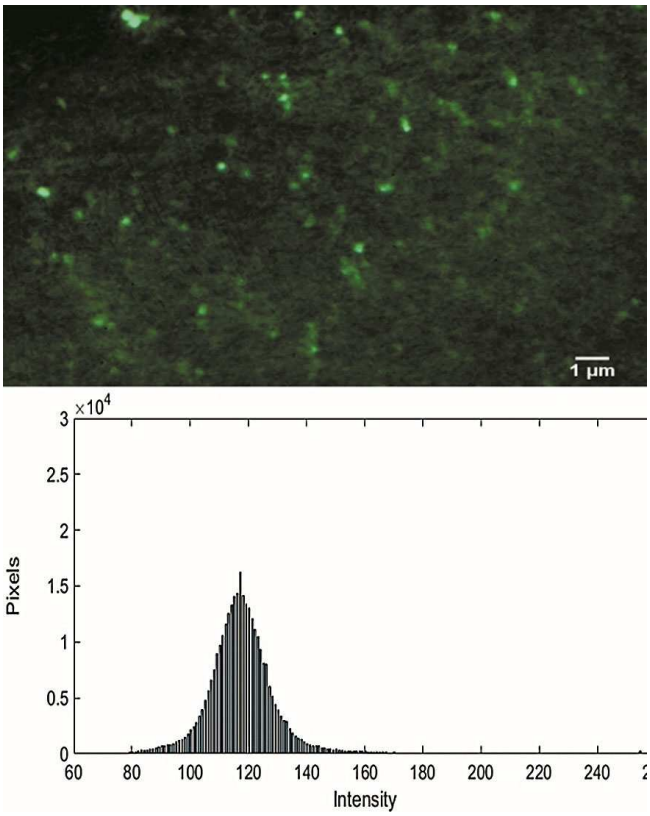

Figure 2. A) Aggregation process monitored by total internal reflection fluorescence microscopy (TIRFM). After 4R maleimide labeling, we observed several oligomers over the glass surface. Scale bar: 1 μm. B) Histogram of pixels intensity shows a graph of the Gaussian function.

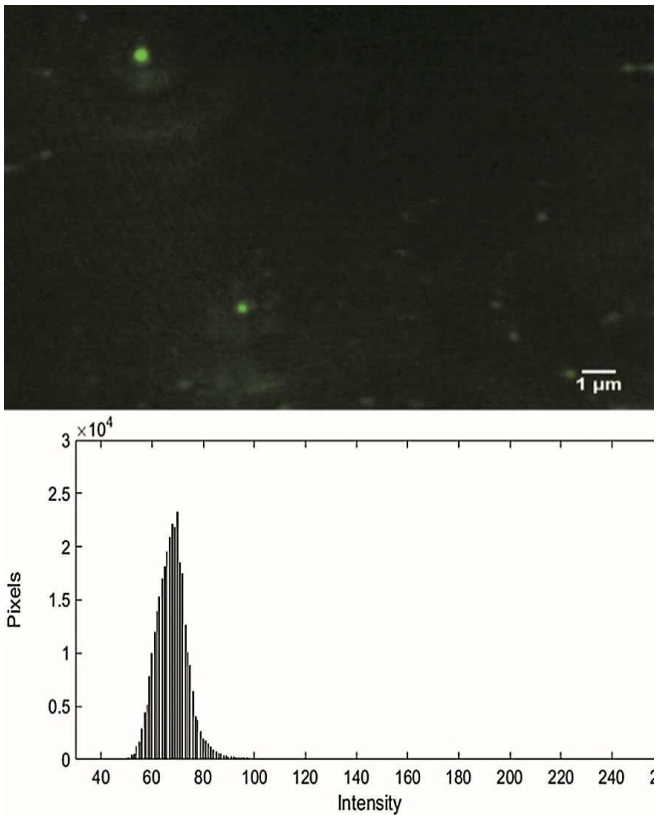

Figure 3. A) Aggregation process monitored by TIRFM in the presence of **2**. After 4R maleimide, we incubated the sample with **2**; later, we observed fewer oligomers over the glass surface. Scale bar: 1 μm. B) Histogram of the treated sample shows a displaced curve to the left indicating fewer pixels intensity.

labeled the Cysteine inside of 4R to monitor the aggregation in presence and absence of **2**. Thus, we observed several oligomers over the glass surface indicating that several oligomers were produced after aggregation induction (Figure 2A). Moreover, when we compared samples treated with **2**, we observed fewer oligomers suggesting that aggregation was not fully completed (Figure 3A). After software analysis we observed a Gaussian distribution of oligomers (Figure 2B) however after treatment we observed displacement of the histogram to the left (Figure 3B) suggesting that were less bright pixels representing fewer oligomers elements

The hallmark of AD and tauopathies are neurofibrillary tangles (NFT) however NFT by themselves are not sufficient to demonstrate cells death and synaptic loss in mice[22] suggesting that soluble oligomers potentially could be more toxic species.[23] Therefore, we decided to test whether after treatment with **2** oligomers were remodeled. Dot blots assays have shown that after induction of aggregation at 48 h, we found marked differences between treated and non-treated oligomers as analyzed, considering that anti-tau (T22) antibody recognizes oligomers but neither fibrils nor monomers, the result suggests that after treatment with naturally occurring compound the oligomers conformation is remodeled as shown (Figure 4A and Figure 4B). Interestingly, the role of cysteine has been described during the progression of tau aggregation by generating toxic tau species.[8,24] Therefore, we decided to test whether the compound **2** could be blocking cysteine-cysteine interaction and subsequent oligomers formation. We observed a large signal after aggregation induction considering that stoichiometry was adapted 1:4 (tau: heparin) as described.[17a] Later, we found that **2** inhibited the aggregation process, this suggests that the inhibition of tau by **2** occurs via interaction with cysteine aminoacidic residues (Figure 4C).

The number of older adults affected worldwide by Alzheimer's disease (AD) is increasing, and unfortunately, there is no definitive treatment.[2,25] AD involved two main proteins such as Aβ and tau protein. However, the deleterious effect of pathological tau protein is more related to dementia.[13a] Moreover, there are several neurodegenerative disorders involving abnormally aggregated tau protein termed as Tauopathies.[4] Interestingly, some evidence is showing that diseases such as dementia with Lewy bodies (DLB), Parkinson's disease with dementia (PDD) and Lewy bodies variant of Alzheimer's disease (LBVAD), where tau protein and α-synuclein co-exist generate pathological synergism.[26] Thus, tau has a leading role in neurodegenerative disorders. Moreover, the tau toxicity not only relies on neurofibrillary tangles but oligomers.[27] Therapeutic strategies against tau involved monoclonal antibodies, kinase inhibitors, microtubule stabilizers and tau inhibitors[28]

Several natural compounds have emerged as tau inhibitors involving non-covalent and covalent interactions.[29] Here we provided evidence that a new naturally compound **2** can inhibit tau aggregation by remodeling tau oligomers. Importantly, we showed that **2** could inhibit tau via Cysteine interaction. Considering that neurodegenerative disorders involving tau only offer palliative treatment for patients, we consider necessary to explore other sources of secondary metabolites where lichens appear as a promising source.

Experimental Section

General Experimental Procedures

TLC was performed on Kieselgel 60 GF254 using n-hexane/EtOAc (6:4 v/v) as mobile phase. TLC spots were visualized by spraying the chromatograms with H_2SO_4–MeOH (5:95, v/v) and heating at 120 °C for 2–3 min. Column chromatography (CC) was performed over Merck Kieselgel 60, particle size 0.063–0.200 mm. All solvents were dried and purified before use according to standard procedures. *E. coli* BL21 (DE3) was used for cloning and expression of tau 4R fragment. Tau recombinant protein purification was done by using a column ProPac IMAC 10 and HPLC system. Labeling of 4R was done by using maleimide Alexa 488. Labeled samples were used for Total internal reflection microscopy and aggregation assays. Dot blots were done using mAb AT-22.

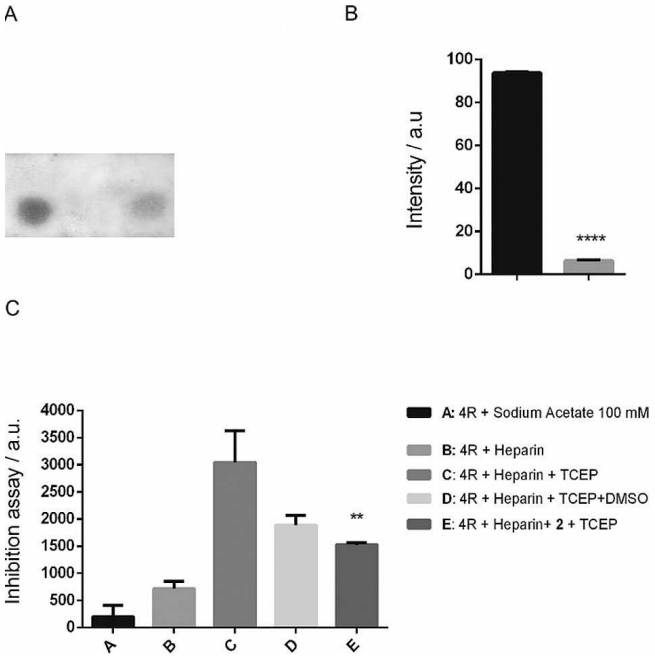

Figure 4. A) Dot blot analysis using mAb AT-22 against oligomer structure of full length tau. Aggregation was started in the presence or not of **2**. B) Fiji analysis of dot blot bands. *P* values were determined by *t student* $P < 0.05$. C) Tau labeled with maleimide-Alexa 488 aggregation induced in the presence and absence of **2**. Dimethyl sulfoxide (DMSO) was used as oxidant control. *P* values were determined by ANOVA with Dunnett Test $P < 0.05$ was considered significant.

Instrumentation

NMR spectra were recorded at 21 °C in acetone-d_6 on a Bruker Avance AM-400 spectrometer operating at 400.13 MHz for hydrogen nucleus. Compounds were individually dissolved in 0.5 ml of deuterated solvent containing tetramethylsilane (TMS) as internal standard. Chemical shifts (δ) were reported in ppm and coupling constants (J) in Hertz. IR spectra were recorded on a Vector 22 FT-IR spectrometer. Mass spectra acquired using a Thermo Finnigan MAT 95XP model spectrometer. Optical rotations were obtained in $CHCl_3$ on a Polax-2L ATAGO, polarimeter.

Plant Material

X. ectaneoides was collected at "Playa de Los gringos" in Constitucion, VII Región, Chile, in 2014. A voucher specimen (N° 100914) was deposited in the Museo Nacional de Historia Natural, Santiago, Chile and Prof. Dr. O. Garcia confirmed the identity.

Extraction and Isolation

Air-dried thalli (20 g) were extracted with EtOAc (room temp., 3 x 100 ml). The organic solution was dried over Na_2SO_4 and the organic solvent was evaporated under reduced pressure yielding an oily extract (200 mg). This extract was submitted to repeated chromatography columns on silica gel using as mobile phase mixtures of n-hexane/EtOAc (9:1 up to 1:9) to yield in order of elution 30 mg of ergosterol peroxide 1[21] and 2 mg of new compound 2. 2-hydroxy-3-((8-hydroxy-3-methoxy-6-methylanthraquinonyl)oxy) propanoic acid (2): gum; $[\alpha]_D^{20} = -32.0$ (c 0.16, $CHCl_3$); FT-IR ν_{max}: 3105–2995, 1435, 1270, 1135 cm^{-1}; HRESIMS (negative mode): m/z 371.0773 [M−H] (calcd. for $C_{19}H_{15}O_8$: 371.0772). ^1H NMR (400 MHz): 2.20 (s, 3H, CH3), 4.02 (s, 3H, OCH3), 4.03 (d, J = 8.3 Hz, 1H, H-1′), 4.84 (brd, J = 4.40 Hz, 1H, H-3′), 5.30 (dd, J = 8.3; 4.4 Hz, 1H, H-2′),6.82 (d, J = 2.5 Hz, 1H, H-7), 7.30 (brs, 1H, H-2), 7.38 (d, J = 2.5 Hz, 1H, H-5), 7.83 (brs, 1H, H-4). ^{13}C NMR (100 MHz): 163.9 (s, C-1), 122.4 (d, C-2), 156.1 (s, C-3), 118.5 (d, C-4), 135.2 (s, C-4a), 107.6 (d, C-5), 166.8 (s, C-6), 109.5 (d, C-7), 168.5 (s, C-8), 115.8 (s, C-8a), 192.3 (s, C-9), 116.7 (s, C-9a), 183.0 (s, C-10), 133.6 (s, C-10a), 70.3 (t, C-3′), 70.3 (d, C-2′), 181.9 (s, C-1′), 57.0 (q, OCH3), 23.8 (q, CH3).

Tau Protein Production

Full length tau and microtubule binding domain4R (htau244-372) were cloned into pET-28a vector (Novagen) to produce a His-tagged protein. The recombinant fragment of full length and 4R was expressed in Escherichia coli strain BL21 (DE3) as described.[30] LB medium containing kanamycin was inoculated with a stationary overnight culture. The culture was grown at 37 °C to OD 600 of 0.5–0.6 and protein expression was induced by addition of 1 mM IPTG for 4 h. The cells were pelleted and sonicated. Recombinant tau was purified via ProPac IMAC 10 (Thermofisher scientific) using a gradient of 10–200 mM imidazole, 20 mM Na_2HPO_4 and 500 mM NaCl. The purity of the protein was verified on a Coomassie Brilliant Blue-stained SDS-polyacrylamide gel. The protein was concentrated and stored at −80 °C until use. The concentration of purified 4R was determined using the extinction coefficient at 280 nm (1520 M^{-1} cm^{-1}).

Thioflavin T Assay

The ThT fluorescence was done as described.[31] Briefly, to examine the inhibition of tau aggregation, the total volume of the reaction mixture was 100 µl, which included 20 µM 4R, 5 µM heparin in

100 mM sodium acetate, pH 6.0 with compound 2. After 48 h of incubation at 37 °C, the addition of 100 µl of a 25 µM solution of ThT and incubated for 1 h at room temperature before fluorescence reading. Then, fluorescence was measured in a Biotek H1 multi-mode reader (Biotek Instruments, Winooski, VT, USA) with an excitation wavelength at 440 nm and emission wavelength at 485 nm in a 96-well plate as described.[30] Each experiment was done at least in triplicate, and background fluorescence was subtracted as needed.

Tau-Alexa 488 Maleimide Labeling

Protein samples were reduced with TCEP (tris(2-carboxyethyl) phosphine) by using a 10 M excess (TCEP 400 µM:4R 40 µM). Then mix was incubated for 2 hs at 37 °C and eluted by using an Amicon Ultra centrifugal filter unit at 3500 rpm for 5 min at 4 °C (Merck Millipore). After that, the protein was incubated with the fluorophore Alexa 488 Maleimide molar ratio (2:1) for 2 hs at 30 °C. The excess of the fluorophore was eluted as described before. The induction of aggregation of protein labeled was done as described.[17a] Briefly, tau protein was induced by adding a molar excess of heparin (1:4) for two hours after that samples were read in a Biotek H1 multi-mode reader in a 96-black plate flat bottom. The Ex/Em was set at 493/516 nm. As oxidant control we include dimethyl sulfoxide (DMSO). Also, these samples were used for TIRF experiments.

Total Internal Reflection Fluorescence Microscopy (TIRFM)

Samples were analyzed in a microscope Olympus IX81 linked to a color camera Pixelink PL-B778F. Briefly, Samples were diluted 1:10 in ultrapure water. Then 5 µl were placed over the coverslips Menzel-Glaser (1,5 x 24 x 60 mm) over Ig TIRF (TIRF LAB). The laser 465 nm was turned on linked to a Side-End Excitation Light Launcher (TIRF LAB) to excite the fluorophore attached to 4R (maleimide Alexa 488, Thermofisher). Then we selected the proper filter (FITC/EGFP/Fluo 3/DiO Acridine Orange(+DNA). The samples were irradiated acquiring images scanning the surface of coverslips by using a software Pixelink Capture OEMa (exposure 250 ms and gain 8 db).

Dot Blot Experiment

Dot blot was developed as described with some modification.[17a] Briefly, 2 µl of full length tau aggregates and full length tau aggregates treated with 2 samples were deposited onto a nitrocellulose membrane, then blocked the strip with 10% milk solution overnight at 4 °C. After that, we washed membrane strip once with 1× TBS low Tween for 5 min. After washing, we incubated the strip with primary antibody anti-tau oligomers T22 (Merck-Millipore) diluted in 5% milk solution for 1 h at room temperature. Then, the strip was washed three times for 5 min in 1× TBS low Tween buffer. Then we incubate the strip with secondary antibodies Goat α-rabbit IgG HRP (diluted 1:2000 in 5% milk solution for 1 h at room temperature. After that, we washed the strip three times for 5 min with 1× TBS low Tween buffer. Then we applied ECL (Thermofisher) following the manufacturer instructions.

Data Analysis

Data analysis was performed using the GraphPad Prism 6.0 and, Sigma plot 12. Data are presented as mean ± SEM and analyzed using either *t*-test or ANOVA. Significance was determined as $P <$ 0.05. Analysis of TIRFM images was performed by using Matlab software.

Acknowledgements

This research was funded by Fondecyt Regular grant number 1150745 to A.C. and C.A. F.M. was funded by Fondecyt Regular grant number 1161010.

Conflict of interest

The authors declare no conflict of interest.

Keywords: tau protein · aggregation · fluorescence · inhibitors · medicinal chemistry

[1] O. L. López, S. T. De Kosky, in *Handbook of Clinical Neurology, Vol. 89*, Elsevier, **2008**, pp. 207–216.
[2] A. S. Association, *Alzheimer's Dementia* **2018**, *14*, 367–429.
[3] C. X. Gong, K. Iqbal, *Curr. Med. Chem.* **2008**, *15*, 2321–2328.
[4] G. Lee, C. J. Leugers, *Prog. Mol. Biol. Transl. Sci.* **2012**, *107*, 263–293.
[5] P. Friedhoff, M. von Bergen, E.-M. Mandelkow, E. Mandelkow, *Biochim. Biophys. Acta Mol. Basis Dis.* **2000**, *1502*, 122–132.
[6] X. Yu, Y. Luo, P. Dinkel, J. Zheng, G. Wei, M. Margittai, R. Nussinov, B. Ma, *J. Biol. Chem.* **2012**, *287*, 14950–14959.
[7] H. L. Zhu, C. Fernandez, J. B. Fan, F. Shewmaker, J. Chen, A. P. Minton, Y. Liang, *J. Biol. Chem.* **2010**, *285*, 3592–3599.
[8] K. Bhattacharya, K. B. Rank, D. B. Evans, S. K. Sharma, *Biochem. Biophys. Res. Commun.* **2001**, *285*, 20–26.
[9] N. Sahara, S. Maeda, M. Murayama, T. Suzuki, N. Dohmae, S. H. Yen, A. Takashima, *Eur. J. Neurosci.* **2007**, *25*, 3020–3029.
[10] G. Ramachandran, E. A. Milan-Garces, J. B. Udgaonkar, M. Puranik, *Biochemistry* **2014**, *53*, 6550–6565.
[11] S. Maeda, N. Sahara, Y. Saito, S. Murayama, A. Ikai, A. Takashima, *Neurosci. Res.* **2006**, *54*, 197–201.
[12] J. Gotz, A. Ittner, L. M. Ittner, *Br. J. Pharmacol.* **2012**, *165*, 1246–1259.
[13] a) F. Kametani, M. Hasegawa, *Front. Neurol. Neurosci.* **2018**, *12*, 25; b) T. M. Inerbaev, A. S. Karakoti, S. V. Kuchibhatla, A. Kumar, A. E. Masunov, S. Seal, *Phys. Chem. Chem. Phys.* **2015**, *17*, 6217–6221; c) W. M. Berhanu, A. E. Masunov, *J. Biomol. Struct. Dyn.* **2015**, *33*, 1399–1411.
[14] K. Hochgrafe, A. Sydow, E. M. Mandelkow, *FEBS J.* **2013**, *280*, 4371–4381.
[15] M. G. Spillantini, T. D. Bird, B. Ghetti, *Brain Pathol.* **1998**, *8*, 387–402.
[16] a) F. Panza, V. Solfrizzi, D. Seripa, B. P. Imbimbo, M. Lozupone, A. Santamato, R. Tortelli, I. Galizia, C. Prete, A. Daniele, A. Pilotto, A. Greco, G. Logroscino, *Immunotherapy* **2016**, *8*, 1119–1134; b) T. Karakaya, F. Fusser, D. Prvulovic, H. Hampel, *Curr. Trends Neurol.* **2012**, *14*, 126–136.
[17] a) S. W. Chua, A. Cornejo, J. van Eersel, C. H. Stevens, I. Vaca, M. Cueto, M. Kassiou, A. Gladbach, A. Macmillan, L. Lewis, R. Whan, L. M. Ittner, *ACS Chem. Neurosci.* **2017**, *8*, 743–751; b) A. Crowe, M. J. James, V. M. Lee, A. B. Smith 3rd, J. Q. Trojanowski, C. Ballatore, K. R. Brunden, *J. Biol. Chem.* **2013**, *288*, 11024–11037.
[18] M. Pickhardt, Z. Gazova, M. von Bergen, I. Khlistunova, Y. Wang, A. Hascher, E. M. Mandelkow, J. Biernat, E. Mandelkow, *J. Biol. Chem.* **2005**, *280*, 3628–3635.
[19] V. Shukla, G. P. Joshi, M. Rawat, *Phytochem. Rev.* **2010**, *9*, 303–314.
[20] E. Stocker-Wörgötter, *Nat. Prod. Rep.* **2008**, *25*, 188–200.
[21] D. B. Sgarbi, A. J. da Silva, I. Z. Carlos, C. L. Silva, J. Angluster, C. S. Alviano, *Mycopathologia* **1997**, *139*, 9–14.
[22] M. Polydoro, C. M. Acker, K. Duff, P. E. Castillo, P. Davies, *J. Neurosci.* **2009**, *29*, 10741–10749.
[23] a) S. M. Ward, D. S. Himmelstein, J. K. Lancia, L. I. Binder, *Biochem. Soc. Trans.* **2012**, *40*, 667–671; b) M. J. Guerrero-Munoz, J. Gerson, D. L. Castillo-Carranza, *Front Cell Neurosci* **2015**, *9*, 464.
[24] Y. Soeda, M. Yoshikawa, O. F. Almeida, A. Sumioka, S. Maeda, H. Osada, Y. Kondoh, A. Saito, T. Miyasaka, T. Kimura, M. Suzuki, H. Koyama, Y.

Yoshiike, H. Sugimoto, Y. Ihara, A. Takashima, *Nat. Commun.* **2015**, *6*, 10216.
[25] D. Brambilla, *Pharm. Res.* **2017**, *35*, 3.
[26] S. Moussaud, D. R. Jones, E. L. Moussaud-Lamodiere, M. Delenclos, O. A. Ross, P. J. McLean, *Mol. Neurodegener.* **2014**, *9*, 43.
[27] C. A. Lasagna-Reeves, D. L. Castillo-Carranza, U. Sengupta, J. Sarmiento, J. Troncoso, G. R. Jackson, R. Kayed, *FASEB J.* **2012**, *26*, 1946–1959.
[28] F. Panza, D. Seripa, V. Solfrizzi, B. P. Imbimbo, A. Santamato, M. Lozupone, R. Capozzo, C. Prete, A. Pilotto, A. Greco, G. Logroscino, *Expert Opin. Pharmacother.* **2016**, *17*, 457–461.
[29] a) A. Cornejo, F. Aguilar Sandoval, L. Caballero, L. Machuca, P. Munoz, J. Caballero, G. Perry, A. Ardiles, C. Areche, F. Melo, *J. Enzyme Inhib. Med. Chem.* **2017**, *32*, 945–953; b) F. I. Baptista, A. G. Henriques, A. M. Silva, J. Wiltfang, O. A. da Cruz e Silva, *ACS Chem. Neurosci.* **2014**, *5*, 83–92; c) P. Velander, L. Wu, F. Henderson, S. Zhang, D. R. Bevan, B. Xu, *Biochem. Pharmacol.* **2017**, *139*, 40–55.
[30] A. Cornejo, J. M. Jimenez, L. Caballero, F. Melo, R. B. Maccioni, *J. Alzheimer's Dis.* **2011**, *27*, 143–153.
[31] A. Cornejo, F. Salgado, J. Caballero, R. Vargas, M. Simirgiotis, C. Areche, *Int. J. Mol. Sci.* **2016**, *17*.

Manuscript received: October 19, 2018